J|A|C|S
ARTICLES

Published on Web 07/01/2010

Expanding the Chemical Versatility of Colloidal Nanocrystals Capped with Molecular Metal Chalcogenide Ligands

Maksym V. Kovalenko,*[,†] Maryna I. Bodnarchuk,[†] Jana Zaumseil,[‡] Jong-Soo Lee,[†] and Dmitri V. Talapin*[,†,‡]

Department of Chemistry, University of Chicago, Illinois 60637 and Center for Nanoscale Materials, Argonne National Laboratory, Argonne, Illinois 60439

Received March 25, 2010; E-mail: mvkovalenko@uchicago.edu; dvtalapin@uchicago.edu

Abstract: We developed different strategies toward the synthesis of colloidal nanocrystals stabilized with molecular metal chalcogenide complexes (MCCs). Negatively charged MCCs, such as SnS_4^{4-}, $Sn_2S_6^{4-}$, $SnTe_4^{4-}$, AsS_3^{3-}, MoS_4^{2-}, can quantitatively replace the organic ligands at the nanocrystal surface and stabilize nanocrystal solutions in different polar media. We showed that all-inorganic nanocrystals composed of metals, semiconductors, or magnetic materials and capped with various MCC ligands can be synthesized using convenient and inexpensive chemicals and environmentally benign solvents such as water, formamide, or dimethylsulfoxide. The development of mild synthetic routes was found to be crucial for the design of highly luminescent all-inorganic nanocrystals, such as CdSe/ZnS and PbS capped with $Sn_2S_6^{4-}$ MCCs, respectively. We also prepared conductive and luminescent layer-by-layer assemblies from inorganically capped colloidal nanocrystals and polyelectrolytes. In close-packed films of 5-nm Au nanocrystals stabilized with $Na_2Sn_2S_6$ we observed very high electrical conductivities (>1000 S cm^{-1}).

1. Introduction

Impressive progress in the chemical synthesis of size- and shape-controlled nanocrystals (NCs) of different metals,[1] semiconductors,[2] and magnetic materials[3,4] has been achieved during the past 15 years. In the present time, intense research efforts are focused on the integration of colloidal nanocrystals into various electronic and optoelectronic devices.[5] The strategies for device fabrication with colloidal NCs have experienced serious challenges caused primarily by the large surface-to-volume ratio inherent to nanoscale materials. Many physical and chemical properties of sub-10 nm NCs are strongly dependent on their surface chemistry. The surface ligands play a key role in the nucleation and growth of colloidal NCs, determine the solubility of NCs in various media through the hydrophilic−hydrophobic balance, and impact the ability of NCs to form long-range ordered assemblies (superlattices).[5] The photophysics,[6,7] charge transport,[8,9] magnetism,[10] and catalytical properties of colloidal NCs[11] all are strongly affected by presence of the surface ligands. The design of competitive functional materials would require transformative efforts invested into the optimization of NC surface chemistry for targeted applications. Recent reports on using colloidal NCs in prototype solar cells,[12−14] photodetectors,[13,15] light-emitting diodes,[16] and field-effect transistors[17] largely benefited from improvements in the capping and linking molecules.

Despite the unbeatable chemical flexibility of organic molecules as capping materials,[5] they have drawbacks typically associated with their highly insulating nature and the instabilities they induce in solid-state devices. Generally, device applications of semiconductors and metals rely on pure, all-inorganic, and usually highly crystalline materials. Previous attempts to completely remove the organic surface ligands damaged the NC properties through the formation of multiple surface dangling bonds and midgap charge-trapping states.[6] The annealing of NC films often leads to the sintering of NCs[18] and generation of undesirable carbonaceous species by partial ligand pyrolysis.[19]

[†] University of Chicago.
[‡] Argonne National Laboratory.

(1) Xia, Y.; Xiong, Y. J.; Lim, B.; Skrabalak, S. E. *Angew. Chem., Int. Ed.* **2009**, *48*, 60–103.
(2) Murray, C. B.; Kagan, C. R.; Bawendi, M. G. *Annu. Rev. Mater. Sci.* **2000**, *30*, 545–610.
(3) Jeong, U.; Teng, X.; Wang, Y.; Yang, H.; Xia, Y. *Adv. Mater.* **2007**, *19*, 33–60.
(4) Sun, S. *Adv. Mater.* **2006**, *18*, 393–403.
(5) Talapin, D. V.; Lee, J.-S.; Kovalenko, M. V.; Shevchenko, E. V. *Chem. Rev.* **2010**, 389–458.
(6) Kuno, M.; Lee, J. K.; Dabbousi, B. O.; Mikulec, F. V.; Bawendi, M. G. *J. Chem. Phys.* **1997**, *106*, 9869–9882.
(7) Pandey, A.; Guyot-Sionnest, P. *Science* **2008**, *322*, 929–932.
(8) Yu, D.; Wang, C.; Guyot-Sionnest, P. *Science* **2003**, *300*, 1277–1280.
(9) Morgan, N. Y.; Leatherdale, C. A.; Drndic, M.; Jarosz, M. V.; Kastner, M. A.; Bawendi, M. *Phys. Rev. B* **2002**, *66*, 075339.
(10) Murray, C. B.; Sun, S. H.; Doyle, H.; Betley, T. *MRS Bull.* **2001**, *26*, 985–991.
(11) Lee, H.; Habas, S. E.; Kweskin, S.; Butcher, D.; Somorjai, G. A.; Yang, P. D. *Angew. Chem., Int. Ed.* **2006**, *45*, 7824–7828.
(12) Gur, I.; Fromer, N. A.; Geier, M. L.; Alivisatos, A. P. *Science* **2005**, *310*, 462–465.
(13) Sargent, E. H. *Adv. Mater.* **2008**, *20*, 3958–3964.
(14) Luther, J. M.; Law, M.; Beard, M. C.; Song, Q.; Reese, M. O.; Ellingson, R. J.; Nozik, A. J. *Nano Lett.* **2008**, *8*, 3488–3492.
(15) Rauch, T.; Boberl, M.; Tedde, S. F.; Furst, J.; Kovalenko, M. V.; Hesser, G. N.; Lemmer, U.; Heiss, W.; Hayden, O. *Nat. Photon.* **2009**, *3*, 332–336.
(16) Caruge, J. M.; Halpert, J. E.; Wood, V.; Bulovic, V.; Bawendi, M. G. *Nat. Photon.* **2008**, *2*, 247–250.
(17) Talapin, D. V.; Murray, C. B. *Science* **2005**, *310*, 86–89.
(18) Ridley, B. A.; Nivi, B.; Jacobson, J. M. *Science* **1999**, *286*, 746–749.
(19) Drndic, M.; Jarosz, M. V.; Morgan, N. Y.; Kastner, M. A.; Bawendi, M. G. *J. Appl. Phys.* **2002**, *92*, 7498–7503.

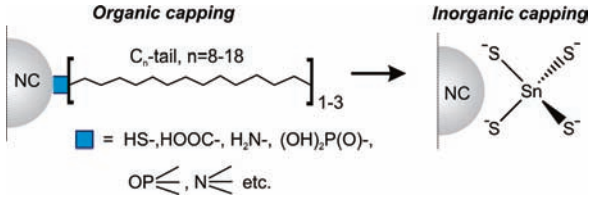

Figure 1. Schematics of the ligand exchange process used for preparation of all-inorganic nanocrystals.

In the search for alternative surface coating, we recently proposed a new class of surface ligands using hydrazine-based metal chalcogenide complexes (N_2H_4-MCCs).[20] To prepare various MCCs, we followed a method developed by D. Mitzi,[21,22] in which the unique solvating and reducing abilities of N_2H_4 were used to dissolve bulk metal chalcogenide and elemental chalcogen and form soluble molecular species of various structural complexity, such as simple ionic $(N_2H_5)_4Sn_2S_6$,[21] 1-dimensional covalent $(N_2H_4)ZnTe$,[23] layered $N_4H_9Cu_7S_4$ complexes,[24] etc. A common feature in N_2H_4-MCCs is the incorporation of hydrazine as either $N_2H_5^+$ counterions or N_2H_4 neutral molecules in the solid form. This enables a unique feature of N_2H_4-MCCs, their easy thermal decomposition to the parent metal chalcogenides.[21,22,25] Decomposed or intact N_2H_4-MCCs show great promise as an "electronic glue" and a functional interparticle medium for NC-based solids,[20] as we demonstrated for highly conductive arrays of Au NCs capped with $(N_2H_5)_2Sn_2S_6$ and for $(N_2H_5)_2Sn_2S_6$-capped CdSe NCs used in field-effect transistors.

The terminal chalcogenide atoms of N_2H_4-MCC ligands have a strong affinity toward binding undercoordinated and electron-deficient metal atoms on the NC surface,[20] suggesting that many other classically bonded metal chalcogenide anions of the main group and transition metals, regardless of the method of their preparation, can be used as the surface ligands. In this work, we report the rational design of all-inorganic NCs using MCCs prepared through alternative and hydrazine-free methods.

Our design of MCC-capped NCs features environmentally benign and air-stable preparations and applicability to NCs which are not chemically compatible with hydrazine or whose properties are strongly altered by the exposure to hydrazine. Using simple methods we prepared main-group metal sulfide MCCs such as Na_4SnS_4, $Na_4Sn_2S_6$, Na_3AsS_3, $(NH_4)_4Sn_2S_6$, and $(NH_4)_3AsS_3$ and used their high affinity to the NC surface to replace commonly used organic ligands (Figure 1). The generality of this approach was demonstrated for a wide range of colloidal NCs including CdS, CdSe, CdSe/ZnS, CdTe, PbS, PbTe, Au, and FePt. We demonstrated that CdSe/ZnS and PbS NCs retain their luminescence properties after the ligand exchange, unlike after treatment with N_2H_4-MCCs. In analogy with N_2H_4-MCCs, complexes with ammonium as the counterion such as $(NH_4)_4Sn_2S_6$ can generate the parent metal chalcogenide (SnS_2) upon mild thermal decomposition at 200 °C. We show that the NC-MCC approach can be extended to transition metal chalcogenide anions such as $(NH_4)_2MoS_4$ as well as to heavier chalcogenide complexes, such as K_4SnTe_4. We also show that the negative surface charge on the NCs arising from adsorbed MCCs can be utilized for electrostatically driven self-assembly with oppositely charged species using the well-known layer-by-layer (LBL) deposition method. Finally, we show that these MCC ligands can support high electrical conductivity in NC solids.

2. Experimental Section

Chemicals. Potassium (99.999%, Aldrich), tin (powder, 99.999%, Alfa Aesar), tellurium (shot, 99.999%, Aldrich), ammonium tetrathiomolybdate ($(NH_4)_2MoS_4$, 97%, Aldrich), sodium sulfide nonahydrate ($Na_2S\cdot 9H_2O$, 99.99%, Aldrich), ammonium sulfide (40−48% solution in water, Aldrich), ammonium hydroxide (28−30% of NH_3, Aldrich), arsenic(III) sulfide (As_2S_3, 99.9%, Alfa Aesar), formamide (FA, 99%, Aldrich), dimethylsulfoxide (DMSO, anhydrous, 99.9%, Aldrich), acetonitrile (anhydrous, 99.8%, Aldrich), and poly(diallyldimethylammonium chloride (PDDA, 20% in water, MW = 100 000−200 000, Aldrich) were used as received. SnS_2 was prepared from $Na_2Sn(OH)_6$ (Aldrich, 95%) and Na_2S as described in the Supporting Information.[26]

Nanocrystal Synthesis. The state-of-the-art synthetic methods were used to prepare organically passivated CdSe, PbS, PbTe, Au, CdTe, FePt NCs and CdS nanorods with or without slight modifications to the original recipes (see Supporting Information for experimental details).[26] CdSe/ZnS and CdSe NCs were also provided by Evident Technologies Inc. (Troy, NY).

Synthesis of Metal Chalcogenide Complexes. Na_4SnS_4 and **$Na_4Sn_2S_6$** were prepared according to the method by Krebs et al.,[27,28] by dissolving SnS_2 in aqueous Na_2S at high pH (pH = 9 for $Na_4Sn_2S_6$ and pH = 11−12 for Na_4SnS_4). $Na_4SnS_4\cdot xH_2O$ and $Na_4Sn_2S_6\cdot xH_2O$ ($x \leq 14$) were precipitated by the addition of acetone, followed by centrifuging and drying. Most of crystalline water can be removed by moderate heating at 100−200 °C. **$(NH_4)_4Sn_2S_6$** was prepared as a 0.1 M solution by dissolving SnS_2 (1 mmol, 183 mg) in a dilute $(NH_4)_2S$ solution (5 mL of H_2O, ~3.2 mmol of $(NH_4)_2S$). The resulting solution was suitable for most of the further experiments. Dry $(NH_4)_4Sn_2S_6$ can be isolated as a yellow powder by the addition of acetone, centrifuging, and drying. The obtained yellow solid slowly decomposes releasing H_2S and, therefore, can be dissolved in water only upon addition of small quantities of $(NH_4)_2S$. **K_4SnTe_4** was prepared according to refs 29 and 30. Briefly, K (1 g) and Sn (3 g) were loaded into a Pyrex tube and heated at 500 °C for 10 h. After cooling, Te powder (4 g) was added to the KSn alloy and the resealed tube was heated at 500 °C for an additional 10 h. The resulting content of the tube was mixed with 12 mL of degassed H_2O forming a dark red solution of K_4SnTe_4 while leaving excessive Sn as a precipitate. Pure K_4SnTe_4 was isolated by vacuum drying and stored in a nitrogen glovebox for further experiments. **$(NH_4)_3AsS_3$**[31] was prepared by dissolving 0.492 g of As_2S_3 in a solution containing $(NH_4)_2S$ (0.86 mL, 40−48% in water) and 10 mL of H_2O at room temepature. **Na_3AsS_3** was prepared in the same way as $(NH_4)_3AsS_3$. The dry Na_3AsS_3 can be isolated by following the same procedure as that for $Na_4SnS_4\cdot xH_2O$.

Exchange of Organic Ligands with Metal Chalcogenide Complexes. The ligand-exchanged NCs were prepared using one of the following protocols. (**Example 1**) Aqueous NH_4OH (8 mL,

(20) Kovalenko, M. V.; Scheele, M.; Talapin, D. V. *Science* **2009**, *324*, 1417–1420.
(21) Mitzi, D. B.; Kosbar, L. L.; Murray, C. E.; Copel, M.; Afzali, A. *Nature* **2004**, *428*, 299–303.
(22) Mitzi, D. B.; Yuan, M.; Liu, W.; Kellock, A. J.; Chey, S. J.; Deline, V.; Schrott, A. G. *Adv. Mater.* **2008**, *20*, 3657–3660.
(23) Mitzi, D. B. *Inorg. Chem.* **2005**, *44*, 7078–7086.
(24) Mitzi, D. B. *Inorg. Chem.* **2007**, *46*, 926–931.
(25) Milliron, D. J.; Raoux, S.; Shelby, R.; Jordan-Sweet, J. *Nat. Mater.* **2007**, *6*, 352–356.
(26) For more details see Supporting information.
(27) Schiwy, W.; Pohl, S.; Krebs, B. *Z. Anorg. Allg. Chem.* **1973**, *402*, 77–86.
(28) Krebs, B.; Pohl, S.; Schiwy, W. *Z. Anorg. Allg. Chem.* **1972**, *393*, 241–252.
(29) Huffman, J. C.; Haushalter, J. P.; Umarji, A. M.; Shenoy, G. K.; Haushalter, R. C. *Inorg. Chem.* **1984**, *23*, 2312–2315.
(30) Korlann, S. D.; Riley, A. E.; Kirsch, B. L.; Mun, B. S.; Tolbert, S. H. *J. Am. Chem. Soc.* **2005**, *127*, 12516–12527.

28−30% of NH_3) was mixed with aqueous $(NH_4)_4Sn_2S_6$ (0.5 mL, ∼0.1 M) or Na_4SnS_4 (1 mL, ∼0.1 M). Hexane (6 mL) and a toluene solution of 3−10 nm CdSe or 6.5-nm CdSe/ZnS NCs (1 mL, ∼25 mg/mL) were added to the aqueous solution, and the mixture was vigorously stirred until the phase transfer of NCs from the organic phase into the aqueous phase was complete. The aqueous phase was rinsed 3 times with hexane. To remove the excess MCC ligands, a minimal amount of acetonitrile was added to precipitate the NCs. The NCs were collected by centrifuging, redispersed in water, and centrifuged/filtered to remove any traces of insoluble materials. (**Example 2**) 6 mL of formamide (FA) were mixed with 0.5 mL of $Na_4Sn_2S_6$ in FA (0.15 M), hexane (6 mL), and 8-nm CdSe NCs in toluene (0.5 mL, 40 mg/mL) and stirred until the phase transfer of CdSe NCs was completed. The FA phase was washed with hexane 3 times, filtered, and mixed with acetonitrile (1:1 v/v) to precipitate NCs. After centrifuging, NCs were redissolved in 5 mL of FA. A similar procedure was also applied for 3−10-nm PbS, 5-nm Au, and 4-nm FePt NCs. (**Example 3**) In a glovebox, 5 mL of FA (vacuum-dried at 100 °C for 2 h) were mixed with 0.5−1 mL of K_4SnTe_4 in FA (0.1 M), 6 mL of anhydrous hexane, and a toluene solution of CdSe, CdTe, or PbTe NCs (1 mL, ∼25 mg/mL) and stirred until the completion of transfer of the NCs into the FA phase. After completion, the organic phase was discarded, and the NC solution was rinsed 3 times with hexane, filtered, and mixed with acetonitrile (1:5 v/v) to precipitate NCs and to remove excessive K_4SnTe_4. The NCs were then redispersed in FA, DMSO, DMF, or methanol.

Layer-by-Layer (LBL) Deposition of MCC-Capped NCs. Quartz or glass substrates were immersed into a fresh piranha solution (3:1 mixture of 98% H_2SO_4 and 30% H_2O_2) for 30 min and rinsed with copious amounts of water. **Caution:** *Piranha solution is highly corrosive and reactive toward organic compounds and must be handled with care.* The substrates were then immersed into a 0.5% aqueous solution of PDDA (pH = 8) for 15 min, rinsed twice in two beakers with fresh portions of deionized (DI) water (30 s for each dipping), and immersed in a NC solution for 15 min, and again rinsed with DI water as above. The deposition procedure was repeated to form 10−30 bilayers of (PDDA/NCs). The concentration of Na_4SnS_4-capped CdSe NCs (or CdSe/ZnS NCs) in water and $Na_4Sn_2S_6$-capped Au NCs in FA was adjusted to 0.5−1 mg/mL, and the pH was kept at ∼11. In the case of Au NCs deposited from FA solutions, pure FA was used in the first rinsing beaker.

Structural and Optical Characterization. Transmission electron microscopy (TEM) of the samples was performed using an FEI Tecnai F30 microscope operated at 300 kV. Thermogravimetric analysis (TGA) was conducted using a Shimadzu TGA-50 thermal analyzer with a heating rate of 5 °C/min under nitrogen. The absorption spectra of the solutions and thin films were collected using a Cary 5000 UV−vis−NIR spectrophotometer. Thin film absorption spectra were obtained by recording transmittance and total reflectance using a DRA 2500 diffuse reflectance accessory (integrating sphere). Photoluminescence (PL) spectra in the region of 300−900 nm were collected using a FluoroMax-4 spectrofluoremeter (HORIBA Jobin Yvon). To measure the absolute quantum yield (QY) for liquid samples emitting in the 500−700 nm range, Rhodamine 6G was used as a standard (QY = 95% in ethanol).[32] The optical density at the excitation wavelength was adjusted to ≤0.1. Near-infrared PL spectra from dropcast films were collected using a 650-nm laser diode as an excitation source. The PL signal was dispersed using a 150-mm Acton spectrometer and measured by an InGaAs camera (Princeton Instruments). Lifetime measurements in the visible spectral region were performed using a QuantaMaster spectrofluorometer equipped with a LaserStrobe fluorescence lifetime module (Photon Technologies International). Fourier-transform infrared (FTIR) spectra were acquired in the transmission mode using a Nicolet Nexus-670 FTIR spectrometer with a resolution of 4 cm^{-1} and averaging over 64 scans. For the measurements, thick films were deposited on CaF_2 crystal substrates (International Crystal Laboratories) by drying concentrated NC solutions. The IR absorbance was normalized to the weight of absorbing material deposited per unit area of the substrate in the form of a uniform film. ^{119}Sn NMR spectra were acquired using a Bruker DRX 400 NMR spectrometer (9.3 T). The spectrometer frequency was set to 149.211 MHz for ^{119}Sn nuclei. The pulse width was set to 8.025 μs, the acquisition time was 1 s, and the number of scans was 10^3−10^4. Spectra were recorded without solvent locking and with no relaxation delays. The line broadening parameter for exponential multiplication was set to 30 Hz. The sample concentration was typically in the range of 0.2−0.5 M. All spectra were referenced to $Sn(CH_3)_4$. DLS and ζ-potential data were collected using a Zetasizer Nano-ZS (Malvern Instruments, U.K.). Colloidal solutions were filled into a quartz cuvette, and the dip cell electrode assembly with Pd electrodes was used to apply an electric field to solution. A typical ζ-potential measurement included several scans of 100 runs each in high-resolution mode. The concentration was optimized for each sample to achieve a >100 kcps count rate and the best signal-to-noise ratio. Elemental analysis by inductively coupled plasma optical emission spectroscopy (ICP-OES) was performed at the Analytical Chemistry Laboratory (ACL) at Argonne National Laboratory. Samples for ICP-OES analysis were prepared by digesting samples in half-concentrated aqua regia or in half-concentrated H_2SO_4/H_2O_2 (3:1).

3. Results and Discussion

On the Chemical Equilibria in Solutions of MCCs in Different Solvents. Various thiostannate ions constitute the majority of MCC ligands used in this work, and they provide a convenient model system for studying MCC-capped NCs. The advantages of these MCCs lie in their facile preparation, simple molecular structure, and high chemical stability. While most structural identifications of chalcogenidostannate ions are performed by single-crystal X-ray diffraction and by Raman spectroscopy of solid samples, we used ^{119}Sn natural abundance NMR spectroscopy as a convenient tool to identify these ions and their chemical transformations in various solution environments (Figures 2, S1).

^{119}Sn NMR spectra of K_4SnTe_4, extracted from the K/Sn/Te alloy, were recorded with several solvents (Figures 2A, S1). The ^{119}Sn chemical shift in $SnTe_4^{4-}$ is solvent dependent due to solvation or ion-pairing effects and is generally observed between −1675 and −1825 ppm.[29,33−38] We found that aqueous and N_2H_4 solutions of K_4SnTe_4 contain exclusively $SnTe_4^{4-}$ anions ($\delta \approx -1663$ ppm and −1817 ppm, respectively). The ^{119}Sn NMR spectrum from FA solution indicates the presence of two anions: $SnTe_4^{4-}$ ($\delta = -1726$ ppm, ∼85%,) and $Sn_2Te_6^{4-}$ ($\delta = -1678$ ppm, ∼15%). ^{119}Sn−^{125}Te spin−spin coupling in $SnTe_4^{4-}$ anions is evidenced by the two satellite peaks with the coupling constant $^1J(^{119}Sn-^{125}Te) \approx 3000$ Hz, which is in good agreement with literature data.[34,37]

(31) Behrens, H.; Glasser, L. *Z. Anorg. Allg. Chem.* **1955**, *278*, 174–183.
(32) Grabolle, M.; Spieles, M.; Lesnyak, V.; Gaponik, N.; Eychmuller, A.; Resch-Genger, U. *Anal. Chem.* **2009**, *81*, 6285–6294.
(33) Burns, R. C.; Devereux, L. A.; Granger, P.; Schrobilgen, G. J. *Inorg. Chem.* **1985**, *24*, 2615–2624.
(34) Campbell, J.; Devereux, L. A.; Gerken, M.; Mercier, H. P. A.; Pirani, A. M.; Schrobilgen, G. J. *Inorg. Chem.* **1996**, *35*, 2945–2962.
(35) Rudolph, R. W.; Wilson, W. L.; Taylor, R. C. *J. Am. Chem. Soc.* **1981**, *103*, 2480–2481.
(36) Teller, R. G.; Krause, L. J.; Haushalter, R. C. *Inorg. Chem.* **1983**, *22*, 1809–1812.
(37) Trikalitis, P. N.; Bakas, T.; Kanatzidis, M. G. *J. Am. Chem. Soc.* **2005**, *127*, 3910–3920.
(38) *Multinuclear NMR*; Mason, J., Ed.; Plenum Press: New York, 1987.

Table 1. Nanocrystals, MCC Ligands, Solvents, and Nonsolvents Used for the Preparation of All-Inorganic MCC-Capped Nanocrystals

nanocrystals	MCC ligands	solvents	nonsolvents
CdSe, CdS, CdSe/ZnS, CdTe, PbS, PbTe, Au, FePt	Na_4SnS_4, $Na_4Sn_2S_6$, K_4SnTe_4, Na_3AsS_3, $(NH_4)_4Sn_2S_6$, $(NH_4)_3AsS_3$, $(NH_4)_2MoS_4$	formamide, H_2O, H_2O:NH_3, dimethylforamide, dimethylsulfoxide	acetonitrile, ethylacetate

Compared to $SnTe_4^{4-}$, thiostannate anions are generally more susceptible to the condensation reactions while their $\delta(^{119}Sn)$ is much less solvent and cation dependent. All assigned chemical shifts are in good agreement, within 1 ppm, with the literature values.[39−45] We found that the dissolution of SnS_2 in aqueous $(NH_4)_2S$ generated a compound with a brutto composition of $N_2H_8SnS_3$ as determined by TGA (Figure S2) and ICP-OES elemental analysis. This compound is unstable in the solid form and appears amorphous in powder XRD. ^{119}Sn NMR of its stable aqueous solution (Figure 2B) revealed the presence of $Sn_2S_6^{4-}$ ($\delta(^{119}Sn) = 56.3$ ppm) along with the traces of mononuclear complexes (SnS_4^{4-} and/or SnS_3^{2-}, $\delta(^{119}Sn) \approx 70-75$ ppm) and an unassigned peak at −60 ppm (presumably $Sn_4S_{10}^{4-}$). A similar ^{119}Sn NMR spectrum with dominant $Sn_2S_6^{4-}$ ion (∼90%) species was obtained for $Na_4Sn_2S_6$ in H_2O (Figure S3). Upon dissolving Na_4SnS_4 in water most of material remains in the *ortho*-thiostannate form (SnS_4^{4-}, $\delta(^{119}Sn) = 68.4$ ppm, Figure 2C), while ∼25% of the anions turned to *meta*-thiostannate SnS_3^{2-} ($\delta(^{119}Sn) = 73.4$ ppm). In agreement with Kanatzidis et al.,[44] FA solutions of Na_4SnS_4 contain only $Sn_2S_6^{4-}$ anions (Figure S4, $\delta(^{119}Sn) = 56.6$ ppm), pointing to the importance of solution equilibria for chemical transformations of chalcogenidostannate ions.

Formation of MCC-Capped Nanocrystals by Ligand Exchange. Table 1 shows the NCs, MCC compounds used as ligands, solvents, and nonsolvents used for the preparation of MCC-capped NCs studied in this work. The NCs were originally capped with various hydrocarbon-based ligands making them soluble in nonpolar organic solvents such as hexane or toluene. Apart from experiments with K_4SnTe_4, all ligand exchange reactions were carried out in air. The ligand exchange was conducted as a heterogeneous reaction in the mixture of two largely or completely immiscible solvents, e.g. hexane−water and hexane−FA, leading to the complete phase transfer of NCs from the nonpolar to the polar phase and the formation of colloidally stable solutions (Figure 3A).

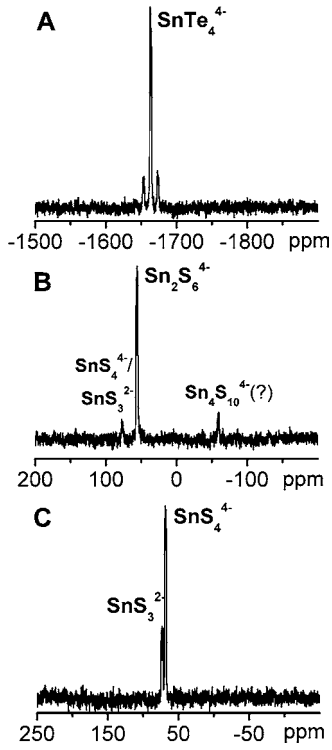

Figure 2. ^{119}Sn NMR spectra of (A) K_4SnTe_4, (B) $(NH_4)_4Sn_2S_6$, and (C) Na_4SnS_4 in aqueous solutions. All spectra were referenced to $Sn(CH_3)_4$.

The time required for complete ligand exchange and phase transfer of NCs ranges from several minutes to several hours and was determined by multiple factors such as the nature of the original organic and the incoming MCC ligands, solvent and solution pH, NC size, etc. As confirmed by TEM studies, the NCs retained their size and shape after the ligand exchange (Figures 3B, S5). The degree of ligand exchange was studied by FTIR spectroscopy. Figure 4A and 4B show FTIR spectra acquired for CdSe/ZnS NCs and CdSe NCs before and after the exchange of the original ligands for Na_4SnS_4 in NH_3/H_2O. The strong absorption lines arising from characteristic C−H and N−H stretching vibrations at 2800−3500 cm^{-1} were replaced with a broad absorption band at 2700−3700 nm^{-1} assigned to the water molecules solvating Na_4SnS_4. The water molecules desorbed under mild heating at 100−200 °C. The rate and completeness of the ligand exchange were very similar to those we previously observed using N_2H_4-MCCs and N_2H_4 as a solvent,[20] which proves that the substitution reaction is mainly driven by the competition between the original organic ligands and the highly nucleophilic MCCs. A very similar behavior was observed for PbS NCs upon exchange of original oleate with AsS_3^{3-} ligands in FA (Figure S6).

ICP-OES elemental analysis of purified 4.1-nm CdSe NCs capped with Na_4SnS_4 provides a S/Sn atomic ratio of ∼4, suggesting the adsorption of intact SnS_4^{4-}. Additionally, we found that the Cd/Sn ratio was 7.1. An approximate estimation of the ligand surface coverage can be made as follows.[46,47] Based on the CdSe NC radius and the bulk CdSe density of 5.81 g cm^{-3}, each NC should contain ∼659 CdSe units. The number of CdSe units within the Cd-Se bond length of 0.263 nm from the NC surface is 223. Thus, the total number of Cd and Se surface atoms is $2 \times 223 = 446$. At the same time,

(39) Dehnen, S.; Zimmermann, C. *Z. Anorg. Allg. Chem.* **2002**, *628*, 2463–2469.
(40) Jiang, T.; Lough, A.; Ozin, G. A.; Bedard, R. L. *J. Mater. Chem.* **1998**, *8*, 733–741.
(41) Jiang, T.; Ozin, G. A.; Bedard, R. L. *Adv. Mater.* **1994**, *6*, 860–865.
(42) Li, J. Q.; Marler, B.; Kessler, H.; Soulard, M.; Kallus, S. *Inorg. Chem.* **1997**, *36*, 4697–4701.
(43) Mundus, C.; Taillades, G.; Pradel, A.; Ribes, M. *Solid State Nucl. Mag.* **1996**, *7*, 141–146.
(44) Rangan, K. K.; Trikalitis, P. N.; Canlas, C.; Bakas, T.; Weliky, D. P.; Kanatzidis, M. G. *Nano Lett.* **2002**, *2*, 513–517.
(45) Ruzin, E.; Zent, E.; Matern, E.; Massa, W.; Dehnen, S. *Chem.−Eur. J.* **2009**, *15*, 5230–5244.
(46) Katari, J. E. B.; Colvin, V. L.; Alivisatos, A. P. *J. Phys. Chem.* **1994**, *98*, 4109–4117.
(47) Jia, S.; Banerjee, S.; Herman, I. P. *J. Phys. Chem. C* **2008**, *112*, 162–171.

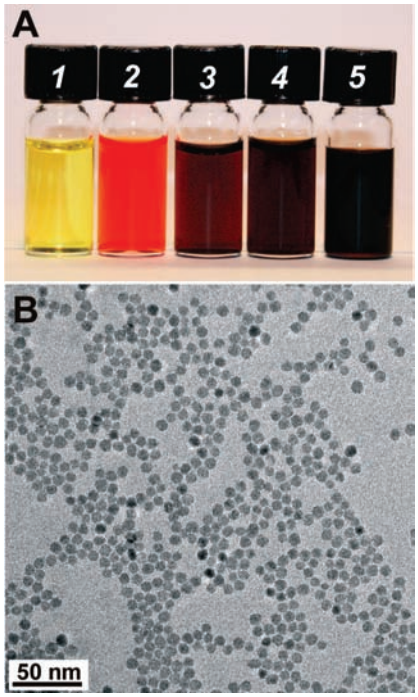

Figure 3. (A) Photographs of stable colloidal solutions formed by various nanocrystal−MCC−solvent combinations: (1) CdS nanorods−$Na_4Sn_2S_6$−formamide, (2) CdSe/ZnS core/shells−Na_4SnS_4−H_2O, (3) Au nanocrystals−Na_3AsS_3−formamide, (4) PbS nanocrystals−$Na_4Sn_2S_6$−formamide, (5) PbTe nanocrystals−K_4SnTe_4−DMSO. (B) TEM image of 8.1 nm CdSe nanocrystals stabilized with K_4SnTe_4 in DMSO.

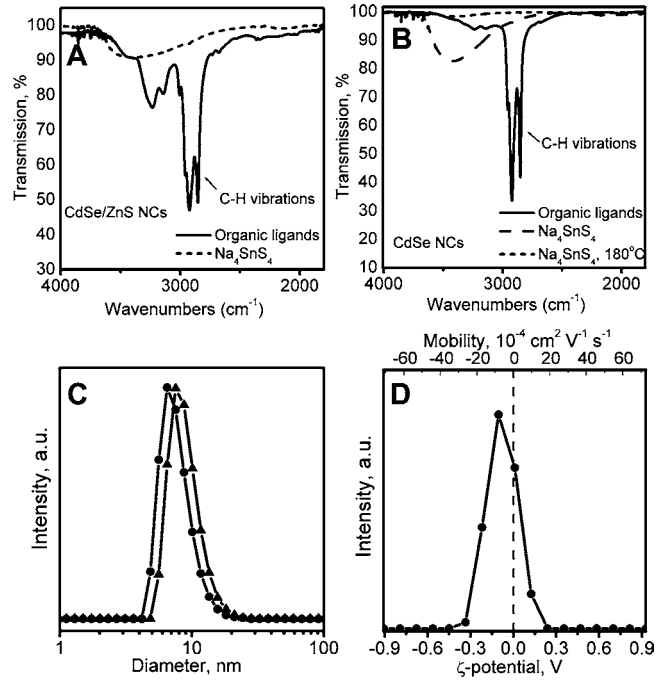

Figure 4. FTIR spectra of (A) 6.5 nm CdSe/ZnS nanocrystals capped with 1-hexadecylamine (HDA) and with Na_4SnS_4 in NH_3:H_2O and (B) 3.8 nm CdSe nanocrystals capped with TDPA−HDA−TOPO and with Na_4SnS_4 in NH_3:H_2O. (C) Size histogram obtained from dynamic light scattering for 6.5 nm CdSe/ZnS nanocrystals stabilized with original HDA ligands (▲) and $(NH_4)_4Sn_2S_6$ (●). (D) Zeta potential (ζ) measured for an aqueous solution of 6.5 nm CdSe/ZnS nanocrystals capped with $(NH_4)_4Sn_2S_6$ ligands.

there are on average 659/7.1 ≈ 93 SnS_4^{4-} ions bound to each NC. Hence the SnS_4^{4-} surface coverage should be 20.8% × *n*, where *n* accounts for the possibility of different binding modes between SnS_4^{4-} species and the NC surface, i.e. the number of Cd surface atoms coordinated with one SnS_4^{4-} ion. For the same NC size but with $(NH_4)_4Sn_2S_6$ as a ligand, we find Cd/Sn = 4.1 and, correspondingly, ∼80 $Sn_2S_6^{4-}$ per one NC, providing similar surface coverage. Note that our NCs are Cd-rich (Cd/Se ≈ 1.3), which is most likely due to a Cd-enriched surface, in agreement with other reports which provided Cd/Se ratios of 1.2 ± 0.15.[46,47]

Colloidal Stability and Solubility. The monomodal size distributions measured by dynamic light scattering (DLS, Figures 4C and S7) indicate that the ligand-exchanged NCs form well-dispersed and aggregate-free solutions. The hydrodynamic diameters are usually similar or slightly smaller than those for the original organic capping, being 7−8 nm for samples shown in Figure 4C, which confirms the adsorption of no more than a single layer of MCC ligands. In agreement with the binding of MCCs to the NC surface, the resulting colloids are electrostatically stabilized in a polar solvent medium. To study the effect of surface charge associated with ionized MCCs on the NC surface, we measured the electrophoretic mobility (μ) of NCs by laser Doppler velocimetry. The electrophoretic mobility is related to the zeta potential (ζ) through the Henry equation, $\mu = 2\varepsilon\zeta f(kr)/3\eta$, where ε is the solvent dielectric constant, η is the solvent viscosity, and $f(kr)$ is Henry's function for a particle with a radius r and the Debye screening parameter k. For aqueous or similar polar media with a moderate electrolyte concentration, a Smoluchowski approximation of $f(kr) = 1.5$ is commonly accepted for estimations of the ζ-potential.[48,49] The magnitude of the ζ-potential corresponds to the electrical potential at a certain plane in the diffuse ionic layer, which is a boundary between mobile and immobilized counterions (shear plane). Closely related to the surface charge and interparticle repulsive potential V_R ($V_R = 2\pi\varepsilon r\zeta^2 \exp(-\kappa D)$, where D is interparticle distance), the ζ-potential allows for the comparison of the colloidal stability of electrostatically stabilized colloids in various polar solvents, regardless of the composition and the precise size and shape of the colloidal particles. The estimated mean ζ-potentials of −50 to −80 mV (Figures 4D, S7) correspond to the high-stability range for electrostatically stabilized colloids, for which a zeta potential of ±30 mV is widely regarded as the borderline between stable and unstable colloids in aqueous or similar media.

The solubility of MCC-capped NCs in various polar solvents is determined by (i) the choice of MCC capping, (ii) the NC core material, and (iii) the pH of the solution. As an example of (i), NCs capped with thiostannate ions are highly soluble (≥20 mg/mL) in high-dielectric constant solvents such as FA and NH_3/H_2O and show a much lower solubility in DMF and DMSO. In comparison, NCs capped with the more polarizable K_4SnTe_4 show excellent solubility in DMSO, DMF, and FA. As an example of (ii), thiostannate-capped CdSe NCs are highly soluble in aqueous NH_3/H_2O (up to 100 mg/mL), while Au and FePt are not. As an example of (iii), the solubility in otherwise "bad" solvents can be significantly altered by increasing the pH (adding NH_3, NaOH, or organic bases), as found for a case of thiostannate-capped CdSe NCs in DMF and DMSO.

Optical Properties of MCC-Capped NCs. CdSe and CdSe/ZnS NCs capped with thiostannate ions in NH_3/H_2O solutions retained their well structured optical absorption spectra (Figure 5A, 5B) with a well resolved lowest $1S_{3/2(h)}-1S_{(e)}$ transition and other electronic transitions at higher energies. As-synthesized oleylamine-capped Au NCs exhibited a pronounced absorption

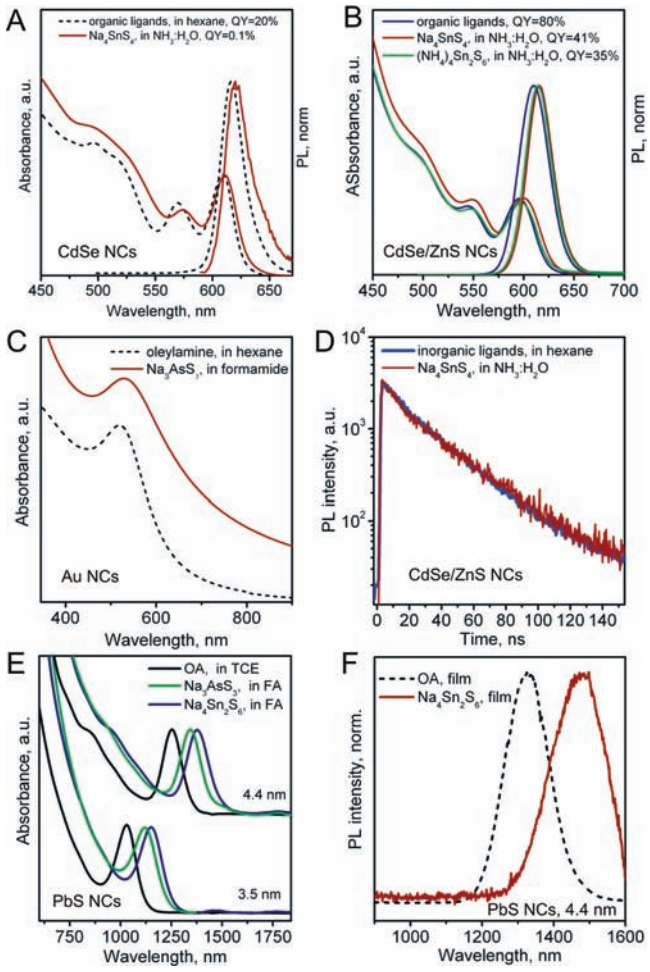

Figure 5. (A) Absorption and photoluminescence spectra for 5.2 nm CdSe nanocrystals capped with original organic ligands (in hexane) and with Na_4SnS_4 (in NH_3:H_2O). (B) Absorption spectra of 6.5 nm CdSe/ZnS nanocrystals capped with organic ligands (in hexane) as well as with Na_4SnS_4 and $(NH_4)_4Sn_2S_6$ (in NH_3:H_2O). (C) Absorption spectra of 5 nm Au NCs capped with oleylamine (in toluene) and with Na_3AsS_3 (in formamide). (D) Fluorescence lifetime measurements of the same solutions of 6.5 nm CdSe/ZnS NCs as shown in (B). (E) Absorption spectra of 3.5 and 4.4 nm PbS nanocrystals capped with oleic acid (OA, in tetrachloroethylene) and with $Na_4Sn_2S_6$ and Na_3AsS_3 (in formamide). (F) PL spectra of films of 4.4 nm PbS NCs capped with oleic acid and with $Na_4Sn_2S_6$.

band due to the surface plasmon resonance (SPR). A slight red shift and broadening of the SPR peak for ligand-exchanged NCs (Figure 5C) is believed to be caused by the change in the dielectric surrounding introduced by the new ligands and solvent.[50]

To better understand the luminescent properties of MCC-capped semiconductor NCs, we analyzed the literature describing the effect of thiols on the luminescence of CdSe-based NCs. Thiols, both short molecules such as thioglycolic acid and longer molecules such as dihydrolipoic acid, completely quench or strongly reduce the photoluminescence (PL) of CdSe NCs.[51−53] Also, the PL of CdSe-based core−shell NCs generally suffers from thiol binding[54−56] and is usually better preserved in samples with multilayer shells composed of CdS, ZnS, and their alloys.[56,57] The PL quenching is generally attributed to the hole trapping by the HOMO level of the thiol lying just above the CdSe $1S_{3/2(h)}$ state.[51] For our CdSe-thiostannate NCs, a significant decrease in the PL QY (typically below 1%) takes place. Such behavior was characteristic for all studied thiostannate ligands in both H_2O and FA. In contrast, CdSe/ZnS core−shell NCs retain their high QY after the surface functionalization with thiostannate ions. The typical QY of 30−45% is similar to the state-of-the-art biocompatible core−shell NCs capped with specially designed capping molecules with multiple SH groups attached to the NC surface (QY = 30−40%).[57] PL lifetime measurements before and after the ligand exchange showed very similar luminescence decay kinetics with radiative lifetimes of 14−16 ns (Figure 5D), confirming the absence of additional nonradiative recombination/trapping pathways.

The effect of the ligand exchange on the optical properties of near-IR emitting PbS NCs was evaluated for two MCC ligands, $Na_4Sn_2S_6$ and Na_3AsS_3, with FA as the solvent (Figure 5E). FA is sufficiently transparent in the near-infrared spectral region up to wavelengths of 1900 nm, and therefore, we have chosen relatively small PbS NCs (3.5 and 4.4 nm) for this study. For both sizes, MCC-capped PbS NCs in FA showed a well resolved excitonic transition without changes in the transition line width and with a pronounced red shift (Figure 5E). For a given ligand, such as $Na_4Sn_2S_6$, the shift is larger for smaller NCs (97 meV vs 66 meV). Such shifts can be explained by the electron and hole wave function leakage into the ligand shell, which is expected from lower energy barriers created by HOMO and LUMO orbitals of MCCs. Films of MCC-capped PbS NCs were highly luminescent (Figure 5F), with a PL intensity of ∼20% relative to the films of oleic acid capped NCs with a similar optical density.

Layer-by-Layer Manipulation with Charged MCC-Capped NCs. Multiply charged species can be used for electrostatically driven adsorption onto various substrates as has been demonstrated for various polyelectrolytes.[58] In this process, known as "LBL assembly", the alternating adsorption of positively and negatively charged species (polymers, short molecules, proteins, colloids, etc.) from their solutions results in the formation of multilayer structures whose thicknesses are proportional to the number of polycation/polyanion bilayers. For more than a decade, this approach has been extensively developed for assembling NC-polyelectrolyte films[59] as well as for all-NC structures.[60] Here we demonstrate this ability for negatively charged MCC-capped CdSe/ZnS, CdSe, and Au NCs NCs by combining them with the commonly used hydrophilic polyca-

(48) O'Brien, R. W.; White, L. R. *J. Chem. Soc. Farad. Trans.* **1978**, *74*, 1607–1626.
(49) Pons, T.; Uyeda, H. T.; Medintz, I. L.; Mattoussi, H. *J. Phys. Chem. B* **2006**, *110*, 20308–20316.
(50) Ghosh, S. K.; Nath, S.; Kundu, S.; Esumi, K.; Pal, T. *J. Phys. Chem. B.* **2004**, *108*, 13963–13971.
(51) Wuister, S. F.; Donega, C. D.; Meijerink, A. *J. Phys. Chem. B* **2004**, *108*, 17393–17397.
(52) Wang, Q. B.; Xu, Y.; Zhao, X. H.; Chang, Y.; Liu, Y.; Jiang, L. J.; Sharma, J.; Seo, D. K.; Yan, H. *J. Am. Chem. Soc.* **2007**, *129*, 6380–6381.
(53) Talapin, D. V.; Rogach, A. L.; Mekis, I.; Haubold, S.; Kornowski, A.; Haase, M.; Weller, H. *Colloid Surf. A-Physicochem. Eng. Asp.* **2002**, *202*, 145–154.
(54) Breus, V. V.; Heyes, C. D.; Nienhaus, G. U. *J. Phys. Chem. C* **2007**, *111*, 18589–18594.
(55) Jiang, Z. J.; Leppert, V.; Kelley, D. F. *J. Phys. Chem. C* **2009**, *113*, 19161–19171.
(56) Dubois, F.; Mahler, B.; Dubertret, B.; Doris, E.; Mioskowski, C. *J. Am. Chem. Soc.* **2007**, *129*, 482–483.
(57) Liu, W.; Howarth, M.; Greytak, A. B.; Zheng, Y.; Nocera, D. G.; Ting, A. Y.; Bawendi, M. G. *J. Am. Chem. Soc.* **2008**, *130*, 1274–1284.
(58) Decher, G. *Science* **1997**, *277*, 1232–1237.

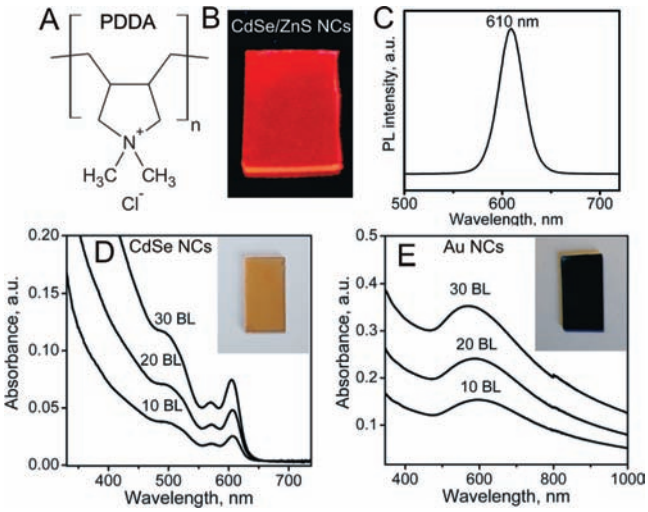

Figure 6. (A) Chemical structure of PDDA. (B) A photograph of {(CdSe)ZnS-Na_4SnS_4/PDDA} × 20 film, assembled from aqueous solutions, taken under UV irradiation. (C) PL spectrum of the film shown in (B). (D) Absorption spectra of {CdSe-Na_4SnS_4/PDDA} × *n* films (*n* is number of bilayers), assembled from aqueous solutions. (E) Absorption spectra of {Au-$Na_4Sn_2S_6$/PDDA} × *n* films, assembled from formamide solutions. Insets show photographs of 30-bilayer thick films.

tion, PDDA (Figure 6A). In all three cases, the optical densities of the obtained homogeneous films scaled with the number of bilayers (Figure 6D, 6E). CdSe/ZnS NCs provided highly luminescent films, with a PL intensity similar to that of close-packed films of CdSe/ZnS NCs of the same optical density. CdSe NCs retain their size-quantized absorption spectra with the peaks at the same wavelengths as in the case of the colloidal solution. From the experiments with Au NCs (Figure 6E), we found that the LBL process can be readily extended to nonaqueous polar solvents, such as FA. The plasmon resonance peak of Au NCs was somewhat shifted with respect to the FA solution, suggesting the regime of weak electronic coupling between individual NCs.

MCC-Capped NCs for Designing Electrically Conductive Solids. Perhaps the most anticipated advantage of using MCC-capping is the improvement of charge transport in solid-state materials composed of all-inorganic NCs.[20] Compared to organic ligands, benefits of MCCs include their smaller size and appropriate HOMO and LUMO energies, leading to the higher "electronic transparency" of the ligand shells. We found that highly conductive films can be obtained for decomposable MCCs containing volatile cations (NH_4^+, $N_2H_5^+$) as well as for nonvolatile cations (Na^+, K^+) ionically bound to chalcogenidometalate anions. Figure 7A shows that the films of Au NCs capped with $Na_4Sn_2S_6$ exhibit very high conductivities of >1000 S cm^{-1}, as opposed to $\sigma \approx 10^{-9}$ S cm^{-1} for Au NCs capped with dodecanethiol molecules. The LBL films of Au NCs contained PDDA spacer molecules which reduced the number of Au NCs in close proximity to each other and, therefore, decreased the conductivity to $\sigma \approx 10^{-2}$ S cm^{-1}.

We further examined the electronic coupling in the arrays of CdSe NCs capped with decomposable $(NH_4)_4Sn_2S_6$. Figure 7B compares the absorption spectra for films of CdSe NCs capped with organic ligands and with $(NH_4)_4Sn_2S_6$ prepared in an aqueous medium. The organically passivated NCs showed

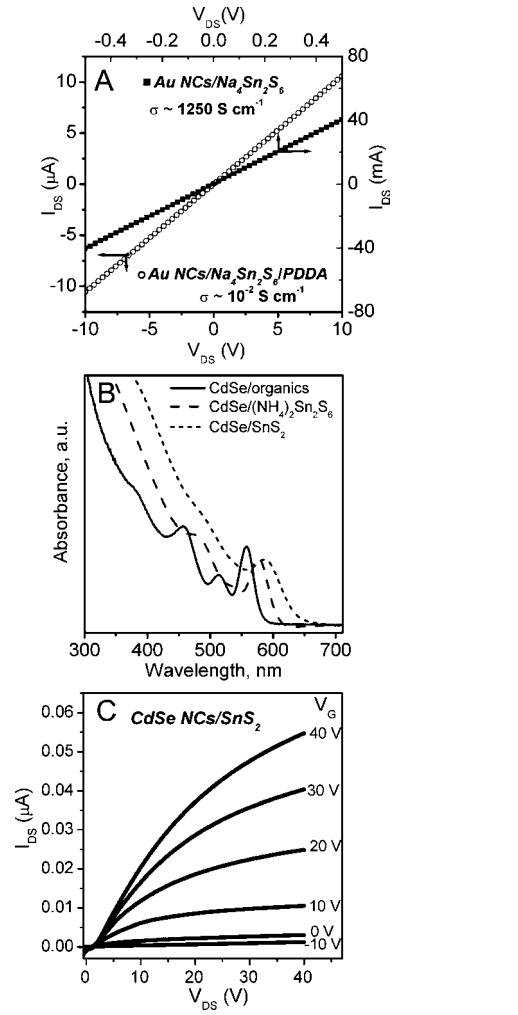

Figure 7. (A) *I*−*V* curves for thin films assembled from 5 nm Au nanocrystals capped with $Na_4Sn_2S_6$ (films were made from the formamide solutions at 80 °C) and for LBL films composed of the same Au/$Na_4Sn_2S_6$ nanocrystals and PDDA. (B) Optical absorption spectra for thin films made from 4.2-nm CdSe nanocrystals capped with the original organic ligands (solid line) and with $(NH_4)_2Sn_2S_6$ before (dash line) and after annealing at 200 °C (short dash line). (C) Plot of the drain current, I_D, versus drain-source voltage, V_{DS}, for a nanocrystal FET with a channel composed of 4.2-nm CdSe nanocrystals capped with $(NH_4)_4Sn_2S_6$ and annealed at 200 °C (channel length is 5 μm, width 7800 μm, 110-nm-thick SiO_2 gate dielectric).

identical spectra in solution and in close-packed films, whereas the absorption spectrum of films of MCC-capped NCs was red-shifted compared to the solution. The absorption features can be further shifted to the red by decomposing ligands at 200 °C: $(NH_4)_4Sn_2S_6 \rightarrow 2SnS_2 + 4NH_3 + 2H_2S$. These results are quantitatively very similar to our previous results for a CdSe NCs−$(N_2H_5)_4Sn_2S_6$ system,[20] showing the improved electronic coupling in the films of MCC-capped NCs. Field-effect transistors (FETs) employing CdSe/SnS_2 NCs as the channel material exhibited pronounced gate modulation of the drain−source current (Figure 7C) with electron mobilities of 1.4×10^{-5} cm^2 V^{-1} s^{-1} (Figure S8A). We also observed an efficient photocurrent generation (Figure S8B), with a secondary photocurrent lasting for minutes, presumably due to the trapping of minority carriers. Using nondecomposable capping such as K_4SnTe_4, we obtained similar charge transport characteristics (Figure S9). For the arrays of PbTe NCs capped with K_4SnTe_4, we observed

(59) Srivastava, S.; Kotov, N. A. *Acc. Chem. Res.* **2008**, *41*, 1831–1841.
(60) Lee, D.; Rubner, M. F.; Cohen, R. E. *Nano Lett.* **2006**, *6*, 2305–2312.

conductivities of 1.9×10^{-2} S cm^{-1} for the as-casted film and $\sigma \approx 2.7$ S cm^{-1} after annealing at 250 °C (Figure S10).

The above-described electrical characteristics were obtained without optimization efforts and can serve only as qualitative evidence of the improved charge transport. The NC films showed numerous structural imperfections such as cracks and pinholes. The film morphologies can be certainly improved for target applications.

4. Conclusions

We demonstrated the general applicability of common chalcogenidometalate compounds for designing functional inorganic cappings for colloidal NCs. This approach benefits from the combination of well established synthetic methodologies for high-quality NCs, the simple and "green" preparation of metal chalcogenide complexes, and the versatility of the ligand exchange. As NC surface ligands, MCCs provide all expected functions: (i) strongly bind to the NC core, (ii) provide colloidal stability of NC solutions, (iii) preserve the electronic structure and photophysics of the NCs, and (iv) add novel and useful functions. MCCs support efficient charge transport in NC solids, as exemplarily shown for Au and CdSe NCs. The described approach provides a very simple route to hydrophilic surface functionality for various NCs, many of which could not be synthesized in water or other polar solvents. Such charged particles are very suitable for electrostatically driven LBL assembly and for designing binary superlattices of oppositely charged particles,[61] as well as for various single-component architectures.[62] Water-soluble particles with small hydrodynamic radii are required for biological luminescent labeling, targeting, and sensing[63] and as contrast agents for magnetic resonance imaging.[64] All-inorganic colloids of MCC-capped NCs can potentially be used as hybrid molecular-nanoparticulate precursors for clean and environmentally benign solution deposition of semiconductors such as synthetic routes for the thermoelectric $Bi_xSb_{2-x}Te_3$[65] and photovoltaic Cu−Zn−Sn−S−Se kesterites[66] that employed toxic, expensive, and air-sensitive hydrazine as a solvent. Despite the several examples of common MCCs used here for a proof-of-principle study, the rich coordination chemistry of chalcogenidometalates[67−71] is likely to provide many more opportunities to be discovered in the near future.

Acknowledgment. We thank B. Lovaasen for PL lifetime measurements and S. Rupich for providing samples of PbS NCs and for reading the manuscript. We thank the Analytical Chemistry Laboratory at Argonne National Laboratory (ANL) for ICP-OES elemental analysis and Evident Technologies Inc. for providing samples of high-quality CdSe and CdSe/ZnS NCs. The work was supported by NSF CAREER under Award Number DMR-0847535 and by the David and Lucile Packard Foundation. The work at the Center for Nanoscale Materials (ANL) was supported by the U.S Department of Energy under Contract No. DE-AC02-06CH11357.

Supporting Information Available: Additional experimental details and figures provided. This material is available free of charge via the Internet at http://pubs.acs.org.

JA1024832

(61) Kalsin, A. M.; Fialkowski, M.; Paszewski, M.; Smoukov, S. K.; Bishop, K. J. M.; Grzybowski, B. A. *Science* **2006**, *312*, 420–424.
(62) Park, S. Y.; Lytton-Jean, A. K. R.; Lee, B.; Weigand, S.; Schatz, G. C.; Mirkin, C. A. *Nature* **2008**, *451*, 553–556.
(63) Medintz, I. L.; Uyeda, H. T.; Goldman, E. R.; Mattoussi, H. *Nat. Mater.* **2005**, *4*, 435–446.
(64) Lee, J. H.; Huh, Y. M.; Jun, Y.; Seo, J.; Jang, J.; Song, H. T.; Kim, S.; Cho, E. J.; Yoon, H. G.; Suh, J. S.; Cheon, J. *Nat. Med.* **2007**, *13*, 95–99.
(65) Kovalenko, M. V.; Spokoyny, B.; Lee, J.-S.; Scheele, M.; Weber, A.; Perera, S.; Landry, D.; Talapin, D. V. *J. Am. Chem. Soc.* **2010**, *132*, 6686–6695.
(66) Todorov, T. K.; Reuter, K. B.; Mitzi, D. B. *Adv. Mater.* **2010**, *22*, E156–E159.
(67) Sheldrick, W. S.; Wachhold, M. *Coord. Chem. Rev.* **1998**, *176*, 211–322.
(68) Dehnen, S.; Melullis, M. *Coord. Chem. Rev.* **2007**, *251*, 1259–1280.
(69) Roof, L. C.; Kolis, J. W. *Chem. Rev.* **1993**, *93*, 1037–1080.
(70) Kanatzidis, M. G.; Huang, S. P. *Coord. Chem. Rev.* **1994**, *130*, 509–621.
(71) Tangirala, R.; Baker, J. L.; Alivisatos, A. P.; Milliron, D. J. *Angew. Chem. Int. Ed.* **2010**, *49*, 2878–2882.